Application of magnetoelastic effects to the evaluation of elastic and plastic strains in steel structural members

Eduard Gorkunov[1,*]

[1]Institute of Engineering Science, RAS (Ural Branch), Ekaterinburg, Russia

Abstract. The paper deals with different methods for evaluating macroscopic and microscopic stresses in ferromagnetic materials by magnetic characteristics. It demonstrates the possibility of reconstructing strain curves according to measured magnetic characteristics of steel products.

1 Introduction

Magnetic methods are successfully used to evaluate the mechanical properties, structural state and phase composition of steel and cast-iron products. Besides the structural state of members, their stress state is of great importance. Macrostresses and induced anisotropy (texture) can be easily revealed by magnetic methods. The evaluation of the level of microstresses is a challenge. The evaluation methods are based on the recording of parameters associated with the displacement of 90° domain walls, that is, with the redistribution of magnetoelastic energy in a ferromagnet.

Under magnetization reversal, the magnetization of ferromagnets changes discretely in the form of irreversible magnetization jumps of different amplitude (the Barkhausen effect). Barkhausen jumps (BJs) appear due to the interaction of domain walls (DWs) with defects of different nature (pores, inclusions, secondary phase precipitations, dislocations, grain boundaries, stress gradients, etc.). Therefore, the recorded BJ flux parameters represent the structural state of ferromagnets, and they are sensitive indicators of its changes, and they can be used both for nondestructive testing and for analysing the degradation of product properties under operation.

2 Evaluation of working macrostresses

Iron-based ferromagnets are characterised by the existence of two subsystems of 180° and 90° domain walls. Figure 1 shows a transition of a 180° domain wall through an inclusion defect in the longitudinal magnetization of an iron-silicon alloy crystal. DW separation from a defect (at a critical field H_{cr}) generates electromagnetic and elastic waves (fig. 1 b).

* Corresponding author: ges@imach.uran.ru

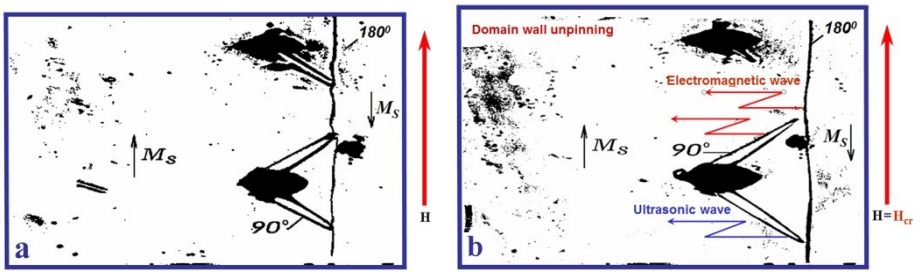

Fig. 1. Interaction of domain walls with an inclusion-type defect.

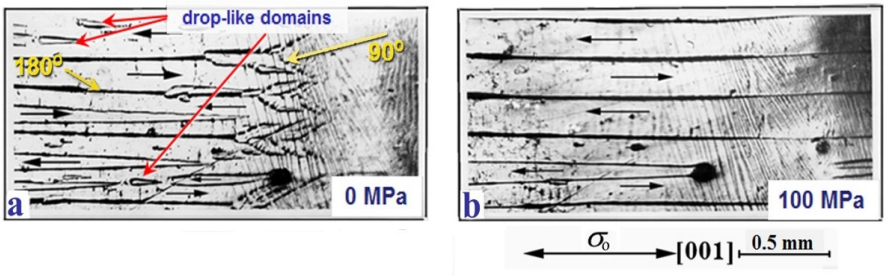

Fig. 2. Rearrangement of 90° domains into 180° ones in silicon iron (a) under 100 MPa tension (b).

A similar process takes place in crystal portions with internal residual stresses. The approach of DWs to these portions causes a jump-like rearrangement of the complex of 90° and 180° domains corresponding to the compression and tension zones [1].

For instance, applied stresses σ_0 change magnetic anisotropy thus reducing the volume of 90° magnetic phases (fig. 2 a, b). At small tensile strains, 90° DWs are substituted by 180° ones; therefore, a texture with magnetization vectors lying along the tetragonal axes closest to the direction of tension is formed in the crystals. The area of 180° DWs grows, and the processes of magnetization reversal become easier.

Thus, in steels with positive magnetostriction ($\lambda>0$) under tension ($\sigma>0$) (positive magnetoelastic effect, $\lambda\sigma>0$) the magnetization reversal processes become easier, whereas under compression (negative magnetoelastic effect, $\lambda\sigma<0$) they are impeded, and this can be illustrated by magnetic hysteresis loops (fig. 3 a) for steel 45.

For nickel, which has negative magnetostriction, the processes of magnetization reversal are more difficult under tension ($\lambda\sigma<0$ – negative magnetoelastic effect), and they are easier under compression (fig. 3 b).

This principle is a basis for the evaluation of working stresses in members made of ferromagnetic materials (fig. 4).

3 Evaluation of the level of microstresses

To evaluate the microstress level in ferromagnetic materials, three approaches are proposed, which involve magnetic energy redistribution in magnetization reversal during the motion of 90° DWs.

One approach involves creating a predominant displacement of 90° DWs, with applied stresses σ_0 in some regions of a ferromagnet being equal to internal ones σ_i. At $\sigma_0 \sim \sigma_i$, the magnetic permeability μ^{90} associated with the displacement of 90° walls is much greater

than that ensuing from the mobility of 180° ones ($\mu^{90} \gg \mu^{180}$). Since the mobility of 90° DWs is governed by the microstress level, the separated contribution of 90° DWs to the process of magnetization reversal enables the microstress level to be evaluated.

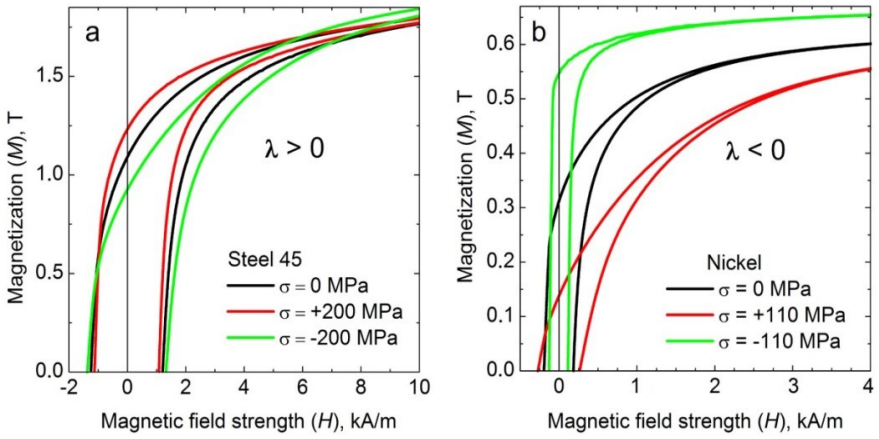

Fig. 3. Hysteresis half-loops for steel 45 (C~0.45%) (a) and nickel (b)

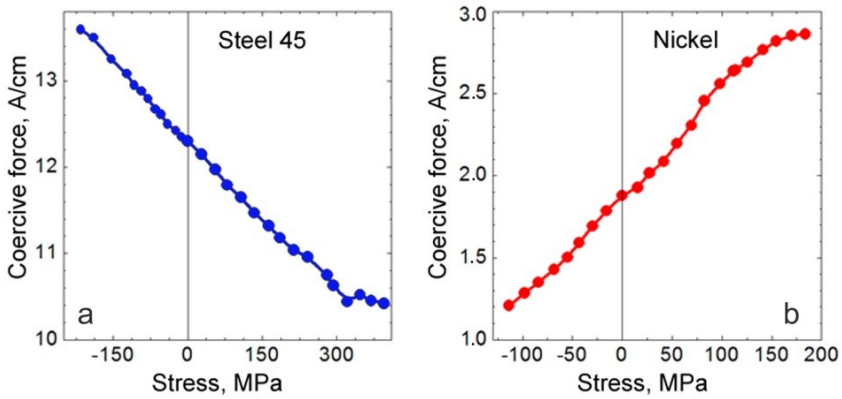

Fig. 4. The coercive force of steel 45 (a) and nickel (b) affected by tensile and compressive stresses

Magnetoelastic studies were conducted as follows (fig. 5): a demagnetized specimen was subjected to tensile stressing (σ_0), then a magnetic field (H) creating induction (B_0) was applied along the tension axis, whereupon low-frequency elastic dynamic vibration of small amplitude ($\Delta\sigma^{\sim}$) was excited in the specimen. The amplitude of magnetic induction ($\Delta B^{\Delta\sigma^{\sim}}$) generated in the specimen by dynamic vibration was recorded by an encircling coil. The measurements were repeated at different tensile loads ranging between 0 and $0.6\sigma_{0.2}$. The plots of measured induction versus tensile loading (fig. 6) have a characteristic form with a peak [2, 3].

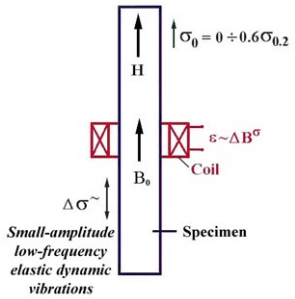

Fig. 5. Experimental scheme.

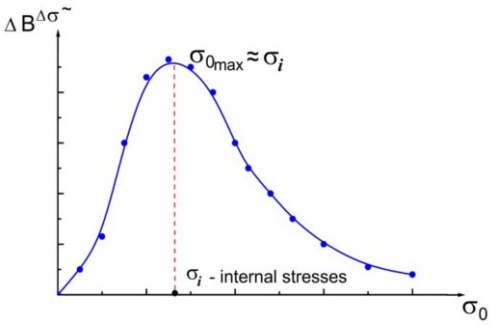

Fig. 6. The behaviour of magnetic induction caused in the specimen by elastic vibrations, $\Delta\sigma^{\sim}$, as a function of applied external stresses.

It follows from [2, 3] that the load value at which the peak is reached correlates with the mean amplitude of internal stresses in differently deformed steels. Thus, according to [2, 3], the value of magnetic permeability μσ associated with the displacement of 90° DWs is determined as

$$\mu^{\sigma} \approx k \frac{\Delta B^{\Delta\sigma}}{\Delta\sigma B_o} \tag{1}$$

Experimental studies demonstrate (fig. 7) that the values of σ_{0max} and μ^{σ} correlate well with dislocation density in iron and steel St3 under plastic deformation.

Another parameter enabling the microstress level in ferromagnetic materials to be estimated is magnetoelastic acoustic emission (MAE). According to current concepts, magnetoelastic acoustic emission is based on the magnetostrictive mechanism of exciting signals produced by local sources of magnetostrictive strain at irreversible displacements of 90° DWs (fig. 1 b) and carrying information about changes in the magnetoelastic state of a ferromagnet.

When a ferromagnetic specimen is affected by an alternating magnetic field, it undergoes magnetization reversal along the magnetic hysteresis loop, and the irreversible displacement of 90° DWs causes elastic wave pulses, (fig. 1 b), which are recorded by a piezotransducer as electric signals. After amplification, the number of jumps of electrical acoustic emission signals is recorded, or the rms values of emf U_{mae} of the envelope of all the jumps are measured. Materials with high values of magnetostriction show high acoustic activity in magnetization reversal.

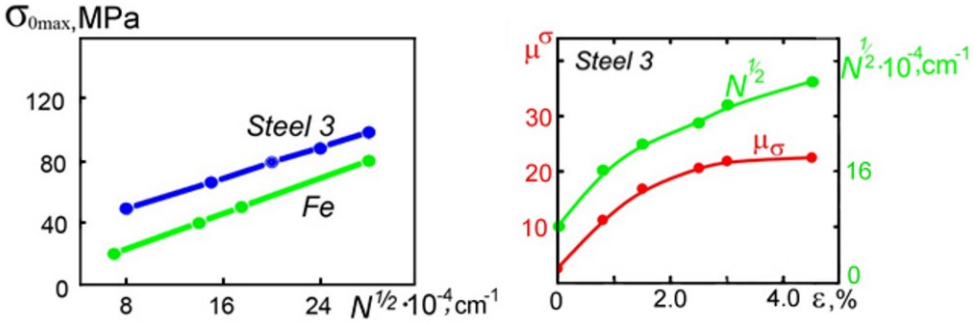

Fig. 7. σ_{0max} and magnetic permeability μ^{σ} caused by the displacement of 90° domain walls as dependent on dislocation density in iron and steel 3 (C~0.2%) suffering plastic deformation

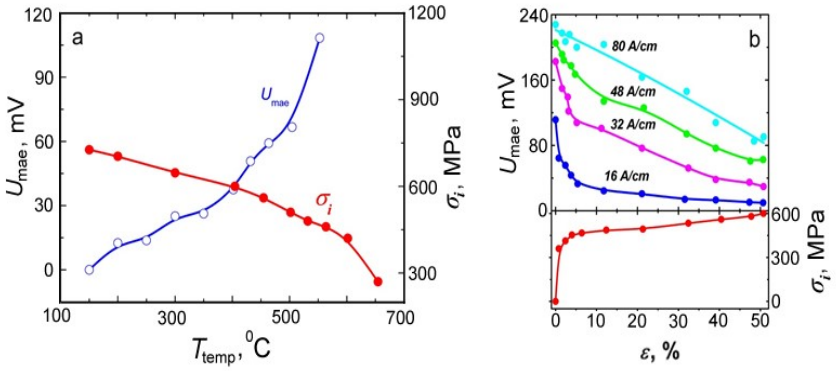

Fig. 8. The behaviour of the rms value of U_{mae} and microstresses as dependent on tempering temperature for steel 34KhN3M (a) and on the amount of plastic strain for steel 40 (b).

As there is a relation between the stress state and magnetostriction, the parameters of magnetoelastic acoustic emission must also be related to the elastic properties of a ferromagnet, i.e., to the microstress level.

Figure 8 illustrates the behaviours of the rms value of U_{mae} and the microstress level as dependent on the tempering temperature for steel 34KhN3M (a) and on the amount of plastic strain for steel 40 (b). It follows from the analysis of fig. 8 that U_{mae} correlates fairly well with the values of microstresses found by the X-ray technique. The MAE technique is employed to evaluate the microstress level in heat-treated and elasto-plastically deformed ferromagnetic materials.

The third approach is magnetostrictive mutual transformation of elastic and electromagnetic waves in ferromagnets, i.e., electromagnetic-acoustic transduction (EMAT). EMAT signal parameters are also sensitive to the microstress level in a ferromagnet.

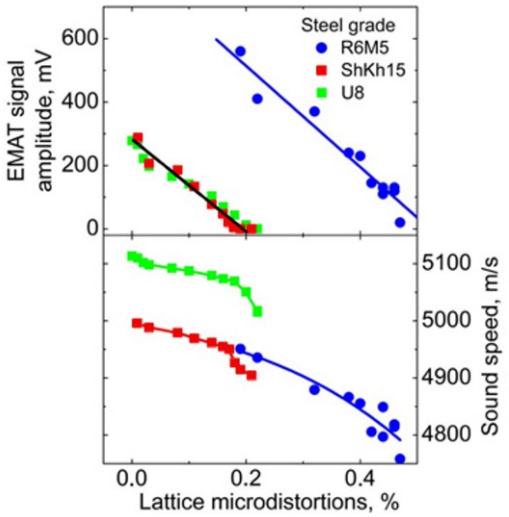

Fig. 9. A relation between the EMAT signal parameters and crystal lattice microdistortions for heat-treated steels.

EMAT in steels was studied in a strong polarizing magnetic field by means of exciting passage coils and recording by the resonance technique to generate a standing elastic wave in the specimen. The EMAT signal amplitude was determined at elastic vibration resonance, as well as the resonance frequency enabling elastic wave propagation velocity to be calculated.

It is obvious from fig. 9 that the EMAT signal amplitude and elastic wave propagation velocity decrease almost linearly with the growth of crystal lattice microdistortions caused by heat treatment (quenching followed by tempering) of specimens made of carbon steel U8 (C≅0.80%; Cr≅0.23%; Mn≅0.22%), low-alloy steel ShKh15 (C≅0.98%; Cr≅1.38%; Mn≅0.32%), high-alloy steel R6M5 (C≅0.84%; Cr≅3.30%; W≅5.92%; V≅1.80%; Mo≅4.83%), and this is suggestive of the applicability of EMAT parameters to the evaluation of the level of microstresses.

4 Reconstruction of strain curves

The determination of the uniaxial stress-strain state of metals by magnetic techniques enables one, using different models of the mechanics of solids, to approach the problem of predicting the behaviour of the mechanical properties of a metal under deformation and evaluating its residual life. It is proposed that magnetic methods of nondestructive testing [4] should be used for monitoring permanent strains in structural members. A technique has been developed for restoring strain diagrams by known relationships of standard mechanical properties of steel and measured magnetic characteristics.

The hardening curve is approximated by the equation

$$\sigma = \sigma_Y + A \cdot \Lambda^n \tag{2}$$

where σ and σ_Y are current working stress and yield stress, $A = (\sigma_U - \sigma_Y)/\Lambda_{sh}^n$, $n = \sigma_U \cdot \Lambda_{sh}/(\sigma_U - \sigma_Y)$, $\Lambda_{sh} = 2 \cdot \ln(1+\delta)/\sqrt{3}$ is shear strain at the end of uniform tension.

If we know correlation between standard mechanical characteristics and magnetic ones, like Y = a+bX, then, after substituting the values obtained from the correlations in eqn. (2), we arrive at a new strain curve equation taking into consideration measured magnetic characteristics, eqn. (3). Thus, by the data obtained in [4], after substituting the correlation expressions $\sigma_Y \approx H_c$, $\sigma_U \approx H_c$ into eqn. (2), we have

$$\sigma = \sigma_Y(H_c) + A(H_c) \cdot \Lambda^{n(H_c)}. \quad (3)$$

The results are presented in fig. 10.

The mechanisms of the strain-induced behaviour of the magnetic characteristics of low- and medium-carbon steels have been experimentally studied on all the portions of the stress-strain diagram up to necking under plane stress conditions in elastic-plastic tensile deformation.

In order to analyse the behaviour of the coercive force in tension, the H_c versus strain curves were superposed on the corresponding stress-strain diagrams (fig. 11). Three characteristic portions are obvious in the behaviour of the coercive force; namely, the region of elastic strain, the yield plateau and/or drop (sharp yield point) and the region of developed plastic strain.

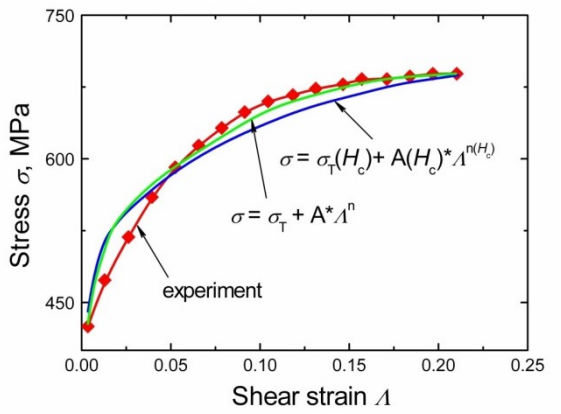

Fig. 10. Experimentally and analytically obtained tension diagrams, eqn. (3).

The effect of stresses reaching and exceeding $\sigma_{0.2}$ leads to a collapse of the magnetic texture of stresses in the elastic strain region, and the coercive force in the plastic strain region is mainly affected by an increase in the density of dislocations and dislocation clusters ($H_c \sim N^{1/2}$, where N is dislocation density [5]) and the formation of a crystallographic strain texture.

As the stress $\sigma_{0.2}$ is approached, the coercive force of all the tested specimens grows significantly, the most active growth of H_c being observed prior to $\sigma_{0.2}$ rather than at $\sigma_{0.2}$, and this agrees well with the results obtained in [6]. In steel St3 the coercive force stops growing as soon as the upper yield stress is reached, H_c remains constant or slightly decreases, and then, after passing the lower yield stress, it resumes growing, though less intensively (see fig. 11 a).

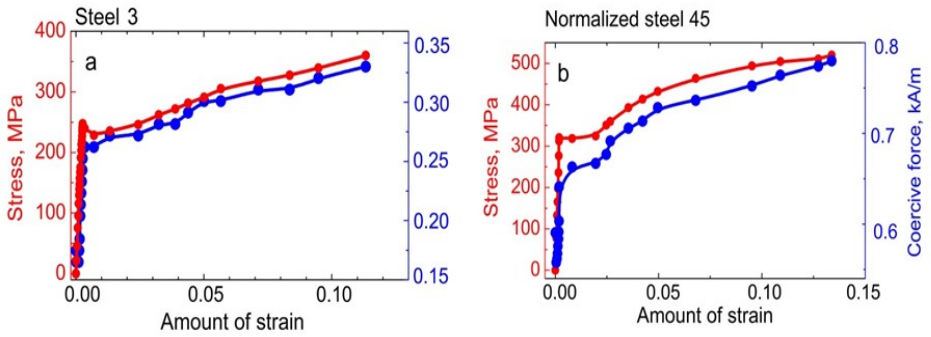

Fig. 11. Tensile stress and coercive force as dependent on the amount of strain for steels.

The investigation has yielded a technique for the restoration of stress-strain diagrams for homogenous steel products by coercive force, and this is a basis for magnetic monitoring of the stress-strain state of loaded steel members.

5 Deformation processes analysed with the use of differential magnetic permeability

To test non-destructively the condition of the constituents of a multilayer product and to assess their residual life, it is suggested that, as was proposed earlier in [7], the value of the field of maximum differential magnetic permeability $H_{\mu dmax}$ of the magnetically soft and magnetically hard constituents of a compound product should be used as an informative parameter. A method for calculating the stress-strain diagram of a flat two-layer steel product under uniaxial tension from the strain-dependences of the magnetic characteristics of the constituents was proposed in [8], the dependences being obtained directly in the course of loading.

Figure 12 a shows the major hysteresis loops of a compound specimen (No. 1 in the table) and its constituents No. 2 and No. 3, both measured separately, as well as the corresponding field dependences of maximum magnetic permeability in the initial state (before loading). The hysteresis loop of the compound specimen (curve 1 in fig. 12 a) has a form characteristic of two-layer ferromagnets [7], and it differs from the hysteresis loops for homogeneous materials (curves 2 and 3), among other things, in that they have two bends. One of them, localized in the region of smaller fields, corresponds to the magnetically soft constituent, and the other corresponds to the magnetically hard one. The mechanism of the formation of these bends was discussed earlier in [5] and [7]. On the field dependence of differential magnetic permeability, bends of the kind manifest themselves as maximums (peaks) of differential magnetic permeability (fig. 12 b). The number of peaks corresponds to the number of layers with different magnetic hardness, the peak height proportion being determined, in particular, by the proportion of the thickness of the respective layers [5, 7].

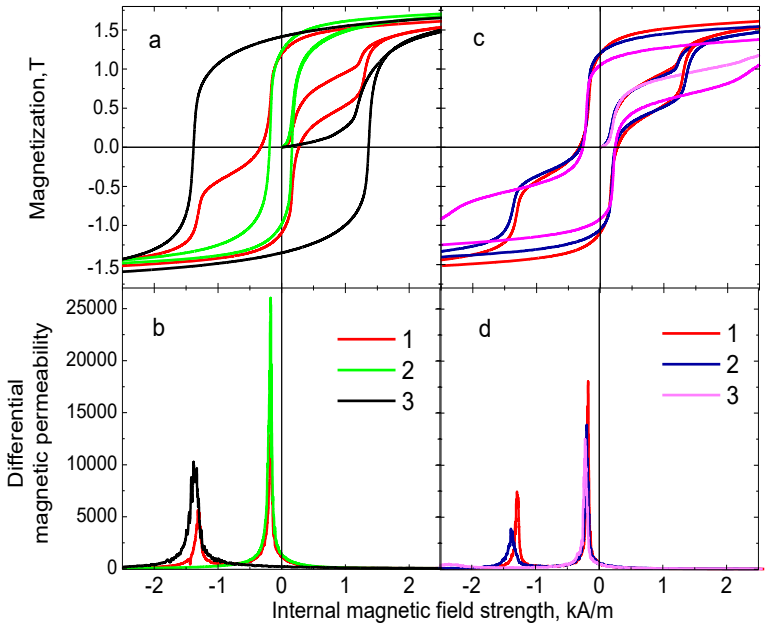

Fig. 12. Major magnetic hysteresis loops for the compound specimen (curve 1) and its constituents (curves 2 and 3) (a) and the corresponding field dependences of differential magnetic permeability (b) in the initial state; for the compound specimen in the initial state (curve 1) (c), under external stresses amounting to 0.5 of the fracture stress in the magnetically hard constituent (2) and immediately before the fracture of the magnetically hard constituent (3).

Table 1. The geometric dimensions of the test parts of the specimens and their magnetic characteristics in the initial state.

No.	Specimen	Dimensions, mm	H_c, kA/m	B_r, T
1	compound specimen: St3+45 (quenching+tempering)	90 × 20 × (2.14+1.10)	0.30	1.14
2	St3 (annealing): 0.03% C, the rest Fe	90 × 20 × 2.04	0.18	1.11
3	45 (quenching+tempering): 0.45% C; the rest Fe	90 × 20 × 1.20	1.36	1.37

Figures 12 c and d show a change in the form of the field dependences of differential magnetic permeability and the evolution of the major hysteresis loops of the compound specimen (No 1). To avoid complication of the figures, we show the curves fitting only three points of the stress-strain diagram; namely, curves 1 correspond to the initial state, curves 2 were taken under external stresses amounting to 0.5 of the fracture stress in the magnetically hard constituent, and curves 3 were obtained immediately before the fracture of the magnetically hard constituent. It follows from fig. 12 c, d that, in the course of deformation, the peak of the magnetically hard constituent on the field dependence of the differential magnetic permeability shifts into the region of stronger fields and, besides, it becomes less intensive and more widened. The peak of the magnetically soft constituent also shifts into the region of stronger fields, due to the small absolute shift magnitude (as compared to that for the magnetically hard constituent), this shift is less pronounced on the

field dependence. The bends of the major loop also shift into the region of stronger fields (see fig. 12 c).

Thus, the field dependences of differential magnetic permeability determined by differentiating the descending branches of the corresponding hysteresis loops with respect to the field reveal the maximums (peaks) of differential magnetic permeability of the individual layers in two-layer products.

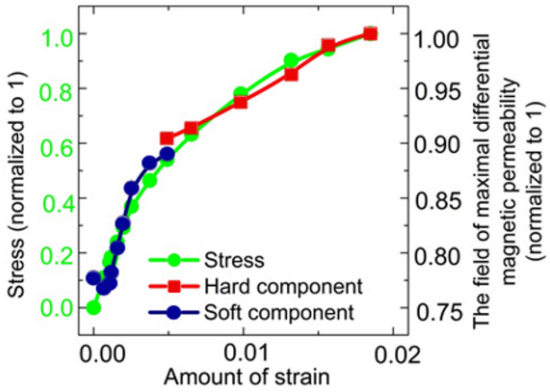

Fig. 13. Tensile stress and the field of differential magnetic permeability as dependent on the amount of strain for a two-layer product.

The characteristics of the peaks of differential magnetic permeability (peak field, height and width) are shown to vary regularly under elastic and plastic strains; therefore, they can serve as a tool for testing the condition of multilayer products. Figure 13 shows a procedure of restoring the stress-strain diagram (green curve) of a two-layer product by its magnetic characteristics. The procedure is based on the following mechanism: when a two-layer product is tensioned, a sharp increase in the value of the field of maximal differential permeability for each constituent occurs under the effect of strains corresponding to the yield stress of the constituent. This enables the strain curve for a two-layer product to be restored – the field $H_{\mu dmax}$ of the magnetically soft constituent is the more informative in the earlier stages of deformation (fig. 13 (o)), whereas $H_{\mu dmax}$ of the magnetically hard constituent is the more informative at higher amounts of strain (fig. 13 (□)).

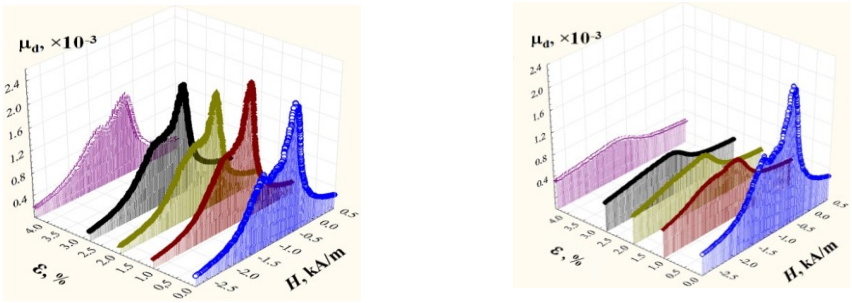

Fig. 14. Evolution of the field dependence of differential magnetic permeability of a laser heat-treated specimen as a function of specific elongation: measurements made under loading (a); measurements made after unloading (b)

Similar results on the change in the field dependence of differential magnetic permeability for carbon steel surface-hardened by laser radiation were obtained for plastic tensile strain (fig. 14).

Conclusion

Magnetic methods are applicable to the evaluation of working macrostresses in structural members. Three techniques for the correlative determination of the level of microstresses in ferromagnetic materials have been discussed. All of them involve the recording of 90° domain wall motion parameters.

A technique for the restoration of stress-strain diagrams of homogeneous steel products by coercive force and/or residual induction has been proposed, which is a basis for magnetic monitoring of the stress-strain state of loaded steel members.

It has been demonstrated that the characteristics of the peaks of differential magnetic permeability (peak field, height and width) vary regularly under the effect of elastic and plastic strains and, therefore they can be an efficient tool for testing the condition of multilayer products. A procedure of restoring the stress-strain diagram of a two-layer product by its magnetic behaviour has been developed. The procedure is based on a discovered regularity, which is as follows: when a two-layer product is tensioned, a sharp increase in the values of the field of maximum differential permeability for each constituent is induced by strains corresponding to the yield stress of the constituent. This enables one to restore the strain curve for a two-constituent product, i.e., $H_{\mu dmax}$ of the magnetically soft constituents is the more informative parameter in the early stages of deformation, whereas $H_{\mu dmax}$ of the magnetically hard constituent is the more informative at higher amounts of strain.

The study was partially financed by the RFBR, project No 16-08-01077.

References

1. E.S. Gorkunov, Y.N. Dragoshanskii, Russ. J. Nondestr. Test. **35,** 6, 409-426 (1999)
2. A.P. Nichipuruk, E.S. Gorkunov, N.I. Noskova, E.G. Ponomareva, FizMM **12**, 81-87 (1992)
3. A.P. Nichipuruk, E.S. Gorkunov, L.D. Gavrilova, L.V. Atangulova, M.V. Degtyarev, B.I. Kamenetskii, L.S. Davydova, T.I. Chashchukhina, L.M. Voronova, Russ. J. Nondestr. Test. **34,** 4, 273-279 (1998)
4. E.S. Gorkunov, A.B. Bukhvalov, A.Z. Kaganovich, S.S. Rodionova, V.N. Durnitskii, Russ. J. Nondestr. Test. **32,** 6, 469-477 (1996)
5. M.N. Mikheev, E.S. Gorkunov, *Magnetic methods of structural analysis and nondestructive testing*. (Nauka, Moscow, 1993)
6. J.M. Makar, B.K. Tanner, J Magn Magn Mater. **184,** 2, 193-208 (1998)
7. E.S. Gorkunov, B.M. Lapidus, A.V. Zagainov, S.A. Voronov, G.Y. Bushmeleva, Russ. J. Nondestr. Test. **7**, 441–446 (1988)
8. E.S.Gorkunov, S.M. Zadvorkin, I.G. Yemelianov, S.Yu. Mitropolskaya, Phys.metals metallog **103**, 6, 624-632 (2007)